CINTAL - Centro de Investigação Tecnológia do Algarve
Universidade do Algarve

MOVIDE

Modeling Visual Detection

First annual report
October 2001

Ulrich Bobinger and Hans du Buf

Vision Laboratory
University of Algarve
Campus de Gambelas – FCT
8000-810 Faro, Portugal

Funded by FCT/POCTI/FEDER, project POCTI/36445/PSI/2000

Work requested by	CINTAL Universidade do Algarve, Campus da Penha, 8000 Faro, Portugal tel:+351-289800131, cintal@ualg.pt, www.ualg.pt/cintal
Laboratory performing the work	VISLAB - Vision Laboratory Universidade do Algarve, FCT, Campus de Gambelas, 8000 Faro, Portugal ubobing@ualg.pt,w3.ualg.pt/ dubuf/vision.html
Project	MOVIDE Modeling Visual Detection
Authors	Ulrich Bobinger and Hans du Buf
Date	October 2001
Number of Pages	12
Abstract	In this first report we explain the work done, notably the data used, the general model and its calibration, as well as first results of predictions of other exprimental data. Using sinewave functions and the CSF, the parameters of the channels of the model are determined. Then, the calibrated model is used to compute predictions for the detection of other functions like disks. Finally, predictions for CSFs, obtained by the superposition of two different functions, are explained. The entire infrastructure in terms of software and programs is ready for finetuning the model in the second year of the project.
Clearance level	UNCLASSIFIED
Distribution list	VISLAB(1), CINTAL(1)

Contents

1 Resumo

Neste primeiro relatório do projecto explicamos o trabalho efectuado, nomeadamente os dados utilizados, o modelo geral e a calibração, bem como primeiros resultados na previsão de dados de outras experiências. Utilizando funções sinusoidais e a CSF (Contrast Sensitivity Function), os parámetros dos canais do modelo são determinados. Depois, o modelo calibrado é utilizado para calcular previsões para a detecção de outras funções como discos. Finalmente, previsões para CIFs (Contrast Interrelation Functions), obtidas com a sobreposição de duas funções diferentes, são explicadas. Toda a infraestrutura em termos de software e programas está pronta para *finetuning* do modelo no segundo ano do projecto.

2 Abstract

In this first report we explain the work done, notably the data used, the general model and its calibration, as well as first results of predictions of other exprimental data. Using sinewave functions and the CSF, the parameters of the channels of the model are determined. Then, the calibrated model is used to compute predictions for the detection of other functions like disks. Finally, predictions for CSFs, obtained by the superposition of two different functions, are explained. The entire infrastructure in terms of software and programs is ready for finetuning the model in the second year of the project.

3 Introduction

The goal of the MOVIDE project is to develop a model of visual pattern detection that is capable to explain many different data sets, including sinewave gratings, squarewave gratings, Bessel functions, disks as well as CIFs measured by the superposition of e.g. disks and Bessel functions. In the first year the exact model is not so important; first the software for model computations, calibrations and predictions must be developed, and results must be plotted using a graphics package. This is the main theme of this report.

We developed all software to test various detection models. The models used so far consist of a filtering stage, for which existing 2D Gabor filter sets have been used. The Gabor filters are defined in the frequency domain and cover all orientations and a frequency range from 0.5 to 20 cpd (cycles per degree). The following steps in the models are rectification and nonlinear pooling over orientation and spatial distribution, as well as over frequencies. The models are calibrated by determining the weight or gain constant of all frequency channels in order to describe elementary CSFs (contrast sensitivity functions).

The calibration can be done with detection data for linear or circular cosine grating data, or for Bessel functions of zero order. As individual subjects differ in their CSF, we took care to find data for CSF calibration, and other data for model predictions, that have always been measured for the same subject. This report shows model predictions for circular disks, linear halfwave rectified sine- and cosine gratings, linear and circular Bessel J_0 functions, as well as subthreshold summation data for different stimulus combinations.

4 Input data

To test different models, we use periodic (grating or Bessel) stimulus data in order to calibrate the model, and at least one different data set from the same subject to test model predictions. Despite the fact that there is a wealth of useful data sets with a good precision, different data sets measured using the same luminance background are rare. We use a set of threshold data for circular grating patterns which cover a frequency range of 0.5 to 20 cpd and incremental/decremental disks with an area between 1 and 1000 min^2 from du Buf (1987). We also use thresholds for Bessel-type stimuli (frequencies between 1 and 6 cpd) and superimposed disks (between 63 and 1000 min^2) from , as well as circular Bessel-type stimuli and horizontal and circular sinewave gratings; the latter were measured this year by the University of Münster Group to support our project. Finally, we calculated predictions for contrast interrelation functions (CIF) of compound sinusoidal gratings of various spatial frequency combinations and four different grating sizes which have been published recently (Meinhardt and Mortensen, 2001).

All input data were generated in the form of 256×256 pixels with 256 gray levels, where the background luminance was set to 128. Bessel J_0 stimuli were calculated using a FORTRAN library (Press et al., 1996). The spatial resolution for all stimuli was set such that one pixel equals one min. of arc, which implies a total visual angle of 4.3 degrees.

5 General model

The stimuli images were convolved with a set of Gabor filters consisting of N_o orientations and N_f frequencies. Gabor kernels are defined in the frequency domain; therefore only 1 FFT of the input image is needed and $N_f \times N_o$ inverse FFTs to calculate the responses. A frequency range between 0.5 and 20 cpd was covered equally on a logarithmic scale. The ratio of the bandwidth σ_f of each kernel and the frequency f_0 was kept constant, with a maximum value of σ_f that could be used without causing aliasing (i.e. $3 \times \sigma_f \simeq dim/4$; where $dim = 256$). The resulting $N_f \times N_o$ complex response images were rectified. Tests with halfwave and fullwave rectification indicated no significant differences between these two methods. In the following step all responses $R(x, y, f, o)$ are nonlinearly pooled using

$$(\sum_p |R_p|^q)^{\frac{1}{q}},$$

which gives a linear sum for $q = 1$ and a maximum detection for $q \to \infty$. Summation over space with the exponent α has a second possible parameter r, which is the radius of the considered area. It appeared to be sufficient to use a diameter of 60 pixels ($\simeq 1°$), which covers foveal vision. $N_o = 8$ orientations were pooled with an exponent β. The order of the summations is not exchangeable; predictions for disks are better with a model that first sums over orientation and than over space. The summation over the frequency channels (exponent γ) comes last, as the responses for all channels are weighted with a gain parameter (g_f) to calibrate the model.

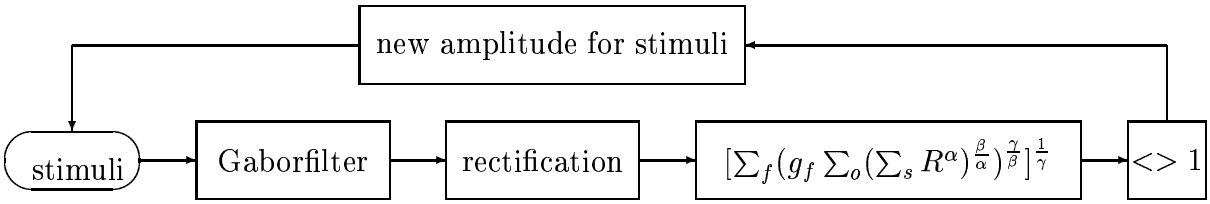

Figure 1: General modeling scheme (f: frequencies (γ); o: orientation (β); s: space (α)). In a calibrated model the final step leads to a detection value of 1.0. As the models are non-linear, bisection at the input is used to reach this value at the output.

6 Model calibration

Figure 2 shows typical approximations of radial sinusoidal CSF and Bessel-type CSF data (the + symbols) which are used to find the system gains g_f. As can be seen, the calibrations obtained are perfect.

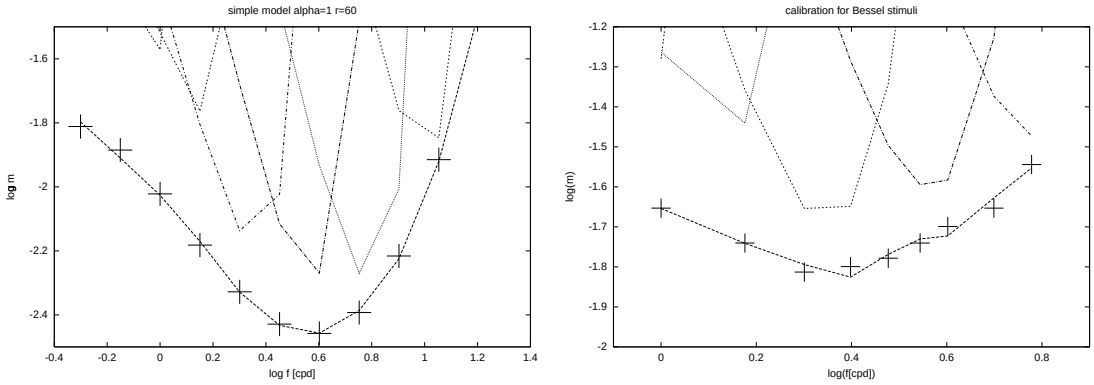

Figure 2: Contrast sensitivity data (+ symbols) for radial sine stimuli (left; data from du Buf, 1987) and radial Bessel stimuli (right; data from Meinhardt and Mortensen, 2001). The graphs include the contributions of individual channels.

7 Different stimuli types

In psychophysical experiments, often either linear gratings or circular ones are used to excitate the channels, i.e. frequency analysers which are tuned to a certain frequency. In the case of a circular disk in the spatial domain, the spectrum is a Bessel $J_0(f)$ function, and vice versa. Therefore, $J_0(f)$ stimuli should excitate all channels having frequencies smaller than f. It is therefore a challenge to make a 2D model that can describe correctly the CSF for all three types of stimuli: linear gratings, circular gratings and Bessel $J_0(f)$ functions. Because the three CSFs, measured with the same experimental conditions and with the same subject, have not yet been published, Günter Meinhardt at the University of Münster measured them in April/May 2001. Figure 3 shows the calibration using normal sinewave grating data (*sin norm* and *fit*), with a few model predictions.

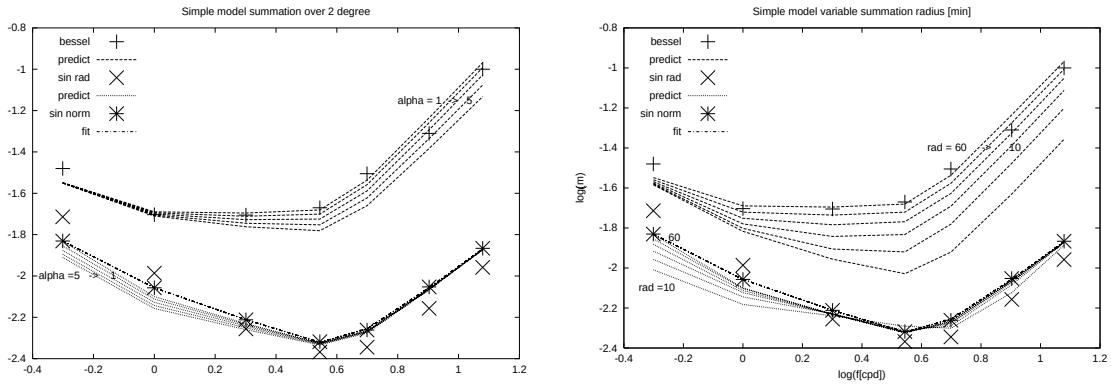

Figure 3: Contrast sensitivity functions for Bessel J_0, radial sine and normal sine stimuli. The graphs show approximations of normal sinusoidal gratings (model calibration) and predictions for Bessel-type and circular sinusoidal stimuli. Data from Günter Meinhardt.

8 Prediction for disks and single-phase gratings

A first test is to see whether the nonlinear model is able to predict threshold data of other stimuli. We therefore calculated approximations for incremental and decremental disks of varying diameter and single-phase rectified gratings, because for these stimuli precise data are available (du Buf, 1987). Figure 4 demonstrates that the rough model is able to produce good predictions for disks with a diameter smaller than about 0.1° and for single-phase gratings with a frequency above 2.5 cpd, but not yet for large disks and low-frequency gratings. To simulate the difference between incremental and decremental disks we simply assumed a smaller negative response at high frequencies by setting $g_f = 0.0$ for channels with $f \geq 10$ cpd. In order to achieve a resolution better than the data points we used a polynomial approximation called *lopsin* (left figure) to calibrate the model (curve *cal*). All predictions in Fig. 4 are calculated with the same parameter set.

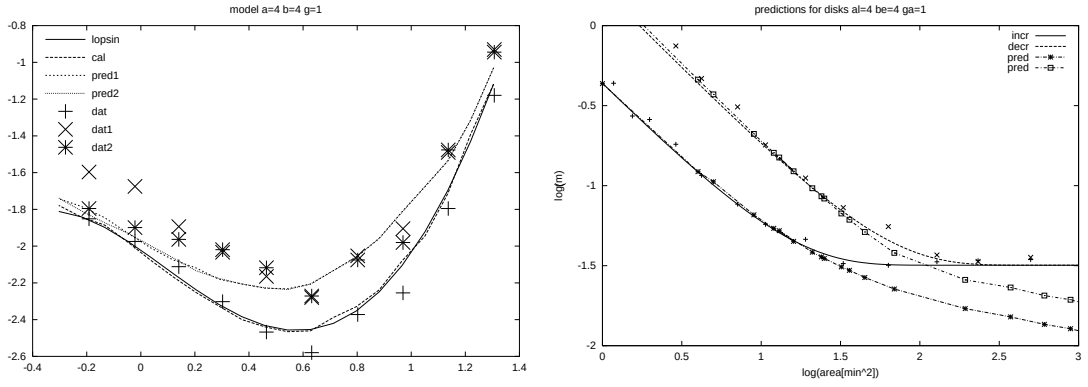

Figure 4: Contrast sensitivity functions for single-phase gratings (left) and incremental and decremental disks (right). Data from du Buf, 1987.

Figure 5 illustrates the flexibility of the model predictions for disks. It can be seen that all predictions for disks with an area larger than 30 min^2 are about 0.3 log units

below the measured data. Model modifications based on different responses for ON and OFF channels, which are now being tested, can hopefully correct this problem.

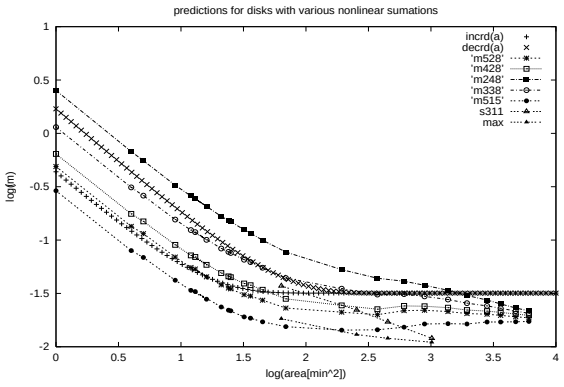

Figure 5: Predictions for threshold contrast of disks; data for increment and decrement luminance from du Buf, 1987. The values of the model parameters α, β and γ are given in the legend by three values, e.g. 528 means $\alpha = 5$. The predictions 's311' and 'max' are based on models that were calibrated using data for Bessel functions (*cal* right) The same two models will be used below for CIFs.

9 Predictions of CIFs for radially symmetric stimuli

Quite recently, CIF data that support the matched-filter model have been published. This concerns the detection of small radially symmetric targets, i.e. disks with an area smaller than 1300 min^2 were superimposed on Bessel $J_0(f)$ functions ranging from 1 to 6 cpd. The CIF technique was introduced by Kulikowski and King-Smith 1973, who stated in the case of a line and a grating: "the change in the contrast threshold for the line due to the subthreshold grating, is a measure of the sensitivity of the line detector to a grating of that frequency." The data points in Fig.6 are the derivatives of the CIF at the point where the contrast of J_0 is zero. In order to estimate the derivatives, positive and negative values of the Bessel functions are used and the CIFs at $(J_0 = 0)$ must be linear. For the model prediction curves we calculated the amplitude that leads to a model response $R = 1$ for five contrast superposition values for each frequency of $J_0(f)$ and each disk size. As can be seen, the rough model can already predict most trends, but lacks precision.

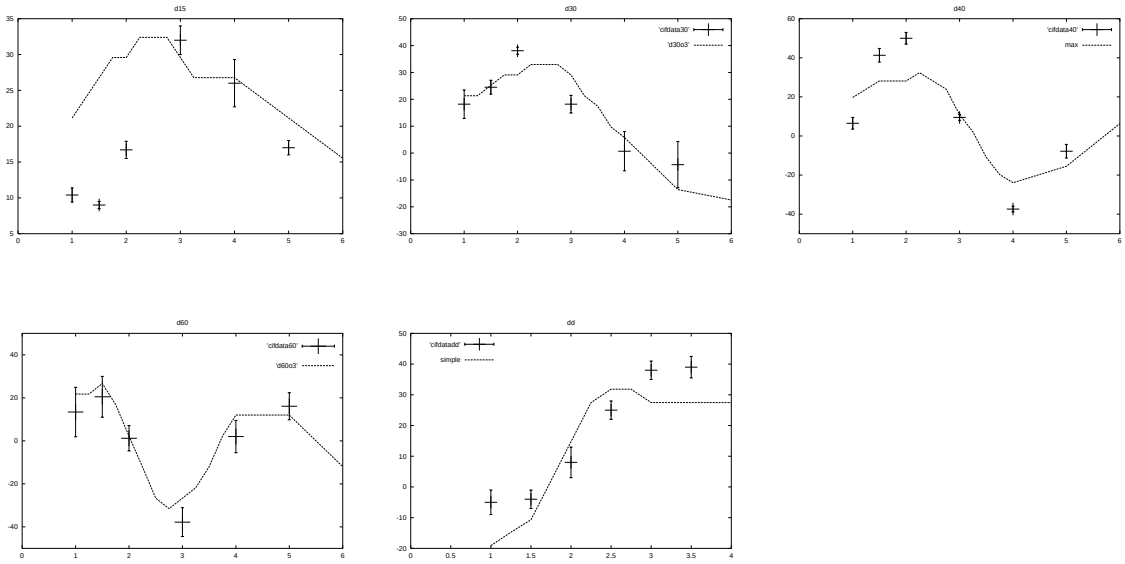

Figure 6: Sensitivity for disks of different diameters, depending on the spatial frequency f (horizontal axis) of a Bessel-type background pattern. Disk sizes are 0.15°, 0.3°, 0.4° (top) 0.6° and a double disk with 0.15° inner and 0.3° outer diameter.

10 Predictions of CIFs for stimuli with different horizontal widths

In the previous section only a very small part of a CIF was used to calculate the sensitivity based on the derivative (slope) of the CIF at one point. New experimental results for superimposed sinusoidal gratings show a variety of different forms in the normalised contrast space, see Meinhardt and Mortensen (2001). In Figs 7-10 the vertical axis represents the normalised contrast m_1 of a sinusoidal grating of 5 cpd and the horizontal axis is m_2 of a superimposed grating having a frequency that is indicated in each panel. The difference between the figures is the horizontal width of the stimuli. All predictions were computed with the same model parameters: $\alpha = 2$, $\beta = 2$ and $\gamma = 5$. The model was calibrated using the CSF of linear sinewave gratings. Each predicted curve consists of 50 threshold calculations. As can be seen from these figures, the model can already predict most of the data, although it has not yet been finetuned.

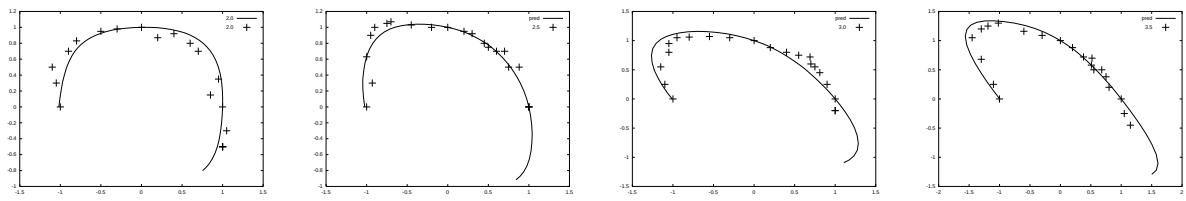

Figure 7: Normalised contrast interrelation functions for a horizontal width of 0.4° and a background grating of 5 cpd. Data points from Meinhardt (2001)

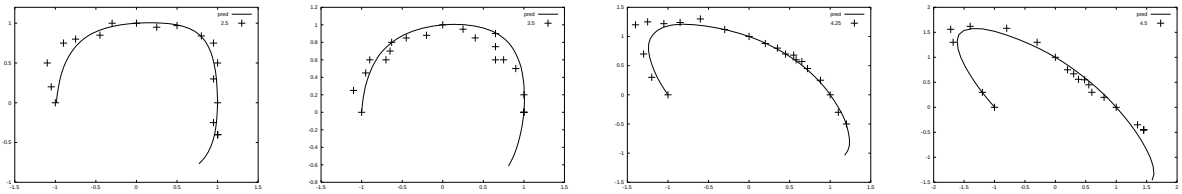

Figure 8: normalized contrast interrelation functions for a horizontal width of 0.8° and a background grating of 5 cpd. Data points from Meinhardt (2001)

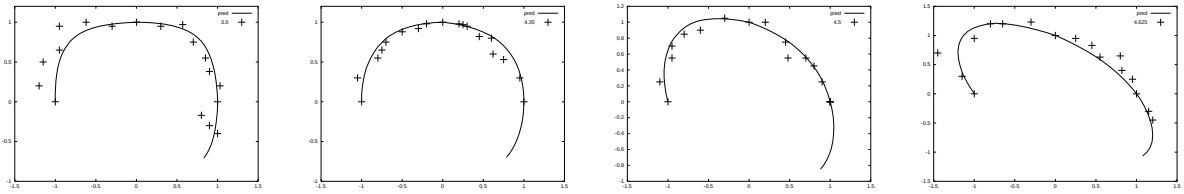

Figure 9: normalized contrast interrelation functions for a horizontal width of 1.6° and a background grating of 5 cpd. Data points from Meinhardt (2001)

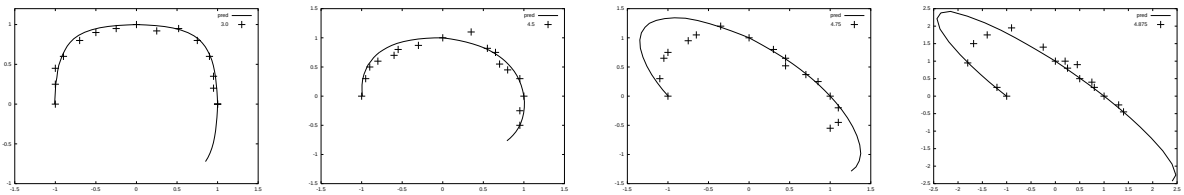

Figure 10: normalized contrast interrelation functions for a horizontal width of 3.0° and a background grating of 5 cpd. Data points from Meinhardt (2001)

11 References

Kulikowski, J.J. and King-Smith, P.E.(1973) Spatial arrangement of line, edge and grating detectors revealed by subthreshold summation, Vision Res., Vol. 13, pp. 1455-1478.

du Buf, J. H. M. (1987) Spatial Characteristcs of Brightness and Apparent-contrast Perception, PhD thesis, Technical University of Eindhoven, the Netherlands.

Press W., Teukolsky S., Vetterling W., Flannery B. (1996) Numerical Recipes in Fortran 77 Cambridge University Press.

Meinhardt, G. and Mortensen, U.(2001) Detection of simple radially symetric targets:further evidence for the matched filter processing scheme in human pattern detection, Biol. Cybern., Vol. 84, pp. 63-74.

Meinhardt G. (2001) Detection of sinusoidal gratings by pattern-specific detectors: further evidence for the correlation principle in human vision. Biol. Cybern., Vol. 85, pp. 401-422.